September 1978 LIDS-P-850

AN OPTIMAL CONTROL APPROACH TO DYNAMIC ROUTING IN DATA COMMUNICATION NETWORKS

PART II: GEOMETRICAL INTERPRETATION

Franklin H. Moss

and

Adrian Segall

This research was supported by the Advanced Research Project Agency of the Department of Defense (monitored by ONR) under contract No. N00014-75-C-1183 and by the Technion Research and Development Foundation Ltd., Research No. 050-383.

The authors were with the Department of Electrical Engineering and Computer Science, M.I.T. Cambridge, Mass. Franklin Moss is now with the IBM Israel Scientific Center, Technion City, Haifa, Israel, and Adrian Segall is with the Department of Electrical Engineering, Technion - Israel Institute of Technology, Haifa, Israel.

Abstract

A continuous state space model for the problem of dynamic routing in data communication networks has been recently proposed. Part I of this series [1] presents the conceptual framework of an algorithm for finding the feedback solution to the associated linear optimal control problem with linear state and control variable inequality constraints when the inputs are assumed to be constant in time. In this paper, a geometrical interpretation of the necessary conditions is presented which facilitates a detailed understanding of several complicating features associated with this algorithm. In Part III, the geometrical interpretation developed here is utilized to derive special properties of the algorithm which lead to a numerical formulation for the case of single destination networks with all unity weightings in the cost functional.

Table of Contents

I. INTRODUCTION

In [2] the minimum delay dynamic message routing problem for data communication networks is expressed as a continuous linear optimal control problem with linear state and control variable inequality constraints. The framework of the Constructive Dynamic Programming Algorithm for building the feedback solution to this problem is presented in Part I of this series [1], for the case in which all the inputs are constant in time. At the end of Section VI of [1] four problems associated with the algorithm are listed which are not confronted in that paper.

The purpose of this paper is to present a geometrical interpretation of the necessary conditions of optimality which assists in the understanding and evaluation of these problems. Although the interpretation is developed within the framework of the Constructive Dynamic Programming Algorithm, its usefulness may be extended to studying fundamental issues regarding the necessary conditions associated with a broad class of linear optimal control problems with linear constraints on the state and control variables.

The organization of the paper is as follows: In Section II, the fundamentals of the geometrical interpretation are derived and the basic theorem which provides the geometrical link between successive steps of the algorithm is presented. The four problems of the Constructive Dynamic Programming Algorithm are discussed in Section III, in the light of the geometrical interpretation. Examples of each of the techniques developed in Section III are presented for specific network problems in Section IV. Discussion and conclusions are found in Section V.

II. GEOMETRICAL INTERPRETATION

We begin with a brief preview of this section. In Part A we consider the pointwise (in time) global linear program of the necessary conditions in the control space as it appears in the space of the state velocity. When viewed in this space in geometrical terms, the cost function at every time is a hyperplane whose coefficients are exactly the costates of the problem at that time. This is a fact which proves advantageous in the attempt to gain insight into the problems of the Constructive Dynamic Programming Algorithm.

In Part B, the pointwise linear program in the control space associated with the constrained optimization problem of the algorithm is also viewed geometrically in the space of the state velocity. The basic advantage to this characterization is the same as described for Part A, only in this case applied to the specific structure of a step of the algorithm. This characterization is in fact detailed for the constrained optimization problems associated with two successive steps of the algorithm, building up to the results of Part C.

In Part C, a theorem is presented which provides an important relationship, expressed in geometrical terms, between successive steps of the algorithm. It is this relationship which sets the stage for the discussion of Section III, also in geometrical terms, of the various problems of the algorithm which are in question.

A. Global Optimization Problem

The necessary conditions associated with the optimal control problem are presented in [1], Theorem 1. They specify that the optimal control at time τ is given by the following linear program in the control space R^m, where m is the dimension of $\underline{u}$, referred to as the *global optimization problem*:

$$\underline{u}^*(\tau) = \text{ARG} \underset{\underline{u}(\tau)\in U}{\text{MIN}} [\underline{\lambda}^T(\tau)\underline{B}\underline{u}(\tau)] \qquad (1)$$

$$\tau \in [t_o, t_f) \ .$$

However, since $\dot{\underline{x}}(\tau)$ is a linear transformation of $\underline{u}(\tau)$ at every τ through the dynamics $\dot{\underline{x}}(\tau) = \underline{B}\underline{u}(\tau) + \underline{a}$ (equation (7) of [1]), we shall gain additional insight into the problem by considering the linear program (1) as it appears in the space of the state velocity. In this spirit the following transformation, induced by the dynamics, is formally defined from the control space R^m to the state velocity space R^n, when n is the dimension of $\underline{x}$:

Definition 1. $\underline{y}(\tau) \triangleq -\dot{\underline{x}}(\tau) = -\underline{B}\underline{u}(\tau) - \underline{a}$

The negative sign has been introduced into Definition 1 as a matter of convenience. Recall that the input vector $\underline{a}$ is taken here to be constant in time. We now define the constrained region in y-space as follows:

Definition 2. $Y \triangleq \{\underline{y} \in R^n / \underline{u} \in U\}$

Since U is a bounded convex polyhedron in R^m then its image Y under the linear transformation of Definition 1 is clearly a bounded convex polyhedron in R^n.

We may now state the global optimization problem (1) as the following linear program in R^n with decision vector $\underline{y}(\tau)$:

$$\underline{y}^*(\tau) = \text{ARG} \underset{\underline{y}(\tau)\in Y}{\text{MAX}} [\underline{\lambda}^T(\tau)\underline{y}(\tau)] \qquad (2)$$

$$\tau \in [t_o, t_f] \ .$$

A particular solution $\underline{y}^*(\tau)$ of (2) is the negative of the optimal state velocity $\dot{\underline{x}}^*(\tau)$ at any point in time.

Unfortunately, an explicit set of linear constraints defining Y is not available in general. Therefore, the most we can hope for from the above definitions is to obtain insights into the problem rather than explicit solutions. As said before, obtaining insights is the purpose of introducing the transformation of Definition 1.

We now proceed with the geometrical interpretation of the global optimization. At each time τ we express the objective function of (2) as the $n-1$ dimensional hyperplane in R^n:

$$H(\tau): \quad Z = \underline{\lambda}^T(\tau)\underline{y} \quad . \tag{3}$$

We refer to $H(\tau)$ as the *global Hamiltonian hyperplane* at time τ since for our problem $\underline{\lambda}^T(\tau)\underline{y}$ is equivalent to the Hamiltonian function of the optimization literature. For a particular value of τ, varying the value of Z causes the Hamiltonian hyperplane to translate parallel to the hyperplane $\underline{\lambda}^T(\tau)\underline{y} = 0$. The optimal solution (s) is achieved for $Z^* = \underline{\lambda}^T\underline{y}$ tangent to Y. The solution set consists of all points of tangency, and may range from a single vertex of Y to an $n-1$ dimensional face of Y.

B. Successive Constrained Optimization Problems

A single step of the Constructive Dynamic Programming Algorithm as described in Section VI of [1] involves allowing the state variables in the set $\mathcal{L}_p$ to leave the boundary backward in time at some imposed boundary junction time t_p. Our goal in this section is to establish a recursive geometrical relationship between *successive* steps of the algorithm. Therefore, we begin the discussion by backtracking one step in the algorithm. Adapting the notation used in [1], this is the situation in which the state variables in $\mathcal{L}_{p+1}$ leave the boundary at t_{p+1}, where t_{p+1} occurs before t_p in the backward sense of time. See Figure 1a.

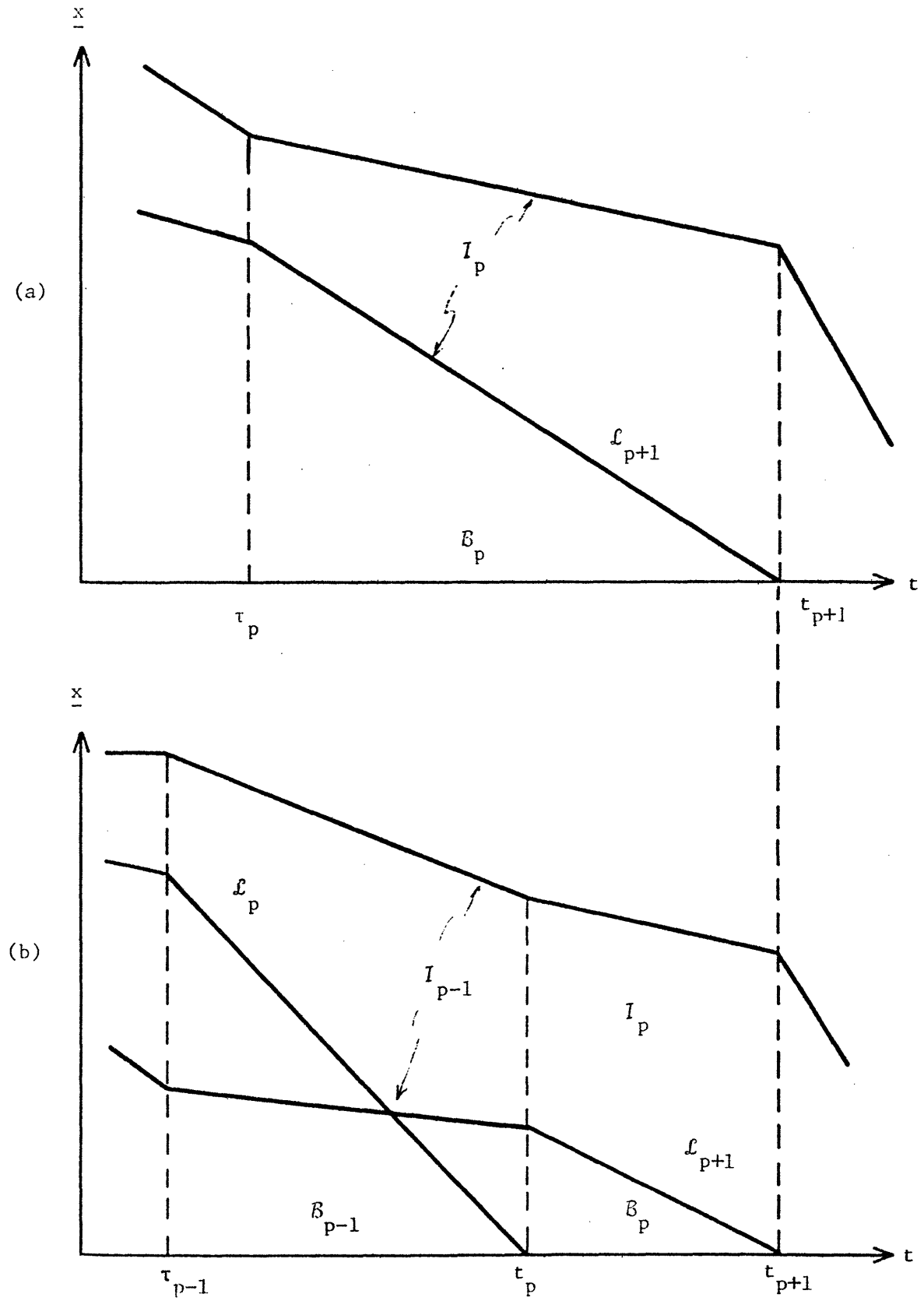

Figure 1 - State variable labelling

Let us now focus attention on Operation 3 of a step of the algorithm (Section VI of [1]) as it applies to the situation under discussion. Part of this operation consists of finding all optimal trajectories on $\tau \in (-\infty, t_{p+1})$ for which $\dot{x}_i^j(\tau) = 0$ for all $x_i^j \in \mathcal{B}_p$, when $\mathcal{B}_p$ is the set of state variables which remain on the boundary immediately after the departure of $\mathcal{L}_{p+1}$ backward in time. In order to actually compute these trajectories, a two part approach is presented in Appendix A of [1]. The *first part* calls for finding all solutions to the following linear program in R^m referred to as the *constrained optimization problem*:

$$\underline{u}^*(\tau) = \text{ARG} \underset{\underline{u}(\tau) \in U}{\text{MIN}} \sum_{x_i^j \in I_p} \lambda_i^j(\tau) \dot{x}_i^j(\tau) \quad [1] \tag{4}$$

subject to

$$\dot{x}_i^j(\tau) = 0 \qquad \forall\, i,j \text{ s.t. } x_i^j \in \mathcal{B}_p \tag{5}$$

$$\tau \in (-\infty, t_{p+1}) \quad ,$$

where I_p denotes the set of state variables which are on interior arcs on $\tau \in (-\infty, t_{p+1})$.

A basic assumption of the algorithm implicit in (4) - (5), and to be discussed later in Section III-D, is that it is optimal for all the members of I_p to remain on interior arcs over this interval. That is, optimality does not dictate that any state variable must return to the boundary backward in time once it has left.

The *second part* consists of determining if there exist values of $\lambda_i^j(\tau)$ for all i,j such that $x_i^j \in \mathcal{B}_p$, $\tau \in (-\infty, t_{p+1})$, so that all solutions

---

1. $\sum_{x_i^j \in I_p}$ shall be used as shorthand notation for $\sum_{i,j \text{ s.t. } x_i^j \in I_p}$

to the constrained optimization (4) - (5) are also solutions to the global optimization (1). Discussion of this part is also deferred until later, Section III-C, where a geometrical test for the existence of these costate values is provided.

Returning attention to the first part, the linear program (4) - (5) in R^m may alternatively be expressed as a linear program in the space R^{σ_p}, where σ_p is the cardinality of I_p and the coordinate axes are y_i^j for all i,j such that $x_i^j \varepsilon I_p$. We begin by defining the appropriate constraint figure:

Definition 3. The σ_p - *dimensional constraint figure* is

$$Y_p \triangleq \{\underline{y} \varepsilon R^{\sigma_p} / \underline{y} \varepsilon Y \quad \text{and} \quad y_i^j = 0 \ \forall i,j \text{ s.t. } x_i^j \varepsilon B_p\} .$$

It is readily seen that Y_p is a bounded convex polyhedron in R^{σ_p} and that

$$Y_p = Y \bigcap R^{\sigma_p} \tag{6}$$

where Y is the global constraint set of Definition 2. The constrained optimization problem of dimension σ_p in y-space is

$$\underline{y}^*(\tau) = \text{ARG} \underset{\underline{y}(\tau)\varepsilon Y_p}{\text{MAX}} \sum_{x_i^j \varepsilon I_p} \lambda_i^j(\tau) y_i^j(\tau) \tag{7}$$

$$\tau \varepsilon (-\infty, t_{p+1}) .$$

As in the case of the global optimization problem, *we are interested in (7) for the purpose of conceptual interpretation rather than for explicit solutions.*

Suppose that we are given a particular set of values of $\lambda_i^j(t_{p+1})$ for all i,j such that $x_i^j \varepsilon I_p$. It is readily seen that solutions to (7) are piecewise constant over time intervals identical to those associated

with the underlying $\underline{u}$-space problem (4) - (5). As in [1], Section VI, we let q denote the number of switches which occur on $\tau \in (-\infty, t_{p+1})$. The time at which these switches occur are denoted $\tau_{p-q+1}, \ldots, \tau_{p-1}, \tau_p$, where the solution remains unchanged from τ_{p-q+1} to minus infinity.[1] The sequence of solution sets to (7) on this time partition is denoted $Y_{-\infty}, Y_{p-q+1}, \ldots, Y_{p-1}, Y_p$ where Y_p applies on $[\tau_p, t_{p+1})$, Y_{p-1} applies on $[\tau_{p-1}, \tau_p)$, ..., and $Y_{-\infty}$ applies on $(-\infty, \tau_{p-q+1})$. Note that $Y_{-\infty}, Y_{p-q+1}, \ldots, Y_{p-1}, Y_p$ are the respective images of the optimal control sets $\Omega_{-\infty}, \Omega_{p-q+1}, \ldots, \Omega_{p-1}, \Omega_p$ (defined in Operation 3, Section VI of [1]) under the transformation of Definition 1. The sets $\Omega_{p-q+1}, \ldots, \Omega_{p-1}, \Omega_p$ are associated with the "break feedback control regions" $R_{p-q+1}, \ldots, R_{p-1}, R_p$ respectively and the set $\Omega_{-\infty}$ is associated with the "non-break feedback control region" $R_{-\infty}$. In general we shall refer to members of the y-space solution sets as σ_p *dimensional operating points.*

The geometric interpretation for the linear program (7) is now given. On every $\tau \in (-\infty, t_{p+1})$ we represent the maximand of (7) as the $\sigma_p - 1$ dimensional hyperplane in R^{σ_p},

$$H_p(\tau): \quad Z = \sum_{x_i^j \in I_p} \lambda_i^j(\tau) y_i^j \quad . \tag{8}$$

We refer to $H_p(\tau)$ as the $\sigma_p - 1$ *dimensional Hamiltonian hyperplane* at time τ. The initial solution set Y_p of the linear program backward in time consists of all points of tangency between Y_p and $H_p(\tau)$ on $\tau \in [\tau_p, t_{p+1})$. See Figure 2. This solution set consists of one or more

---

1. To avoid confusion which could arise in subsequent discussions in this paper, we use notation which distinguishes clearly between switch times which correspond to imposed boundary junction times (e.g. t_{p+1} here) and those corresponding to switches which occur backward in time in the absence of additional state variables leaving the boundary (e.g. $\tau_{p-q+1}, \ldots, \tau_{p-1}, \tau_p$ here). This differs slightly from the notation of [1].

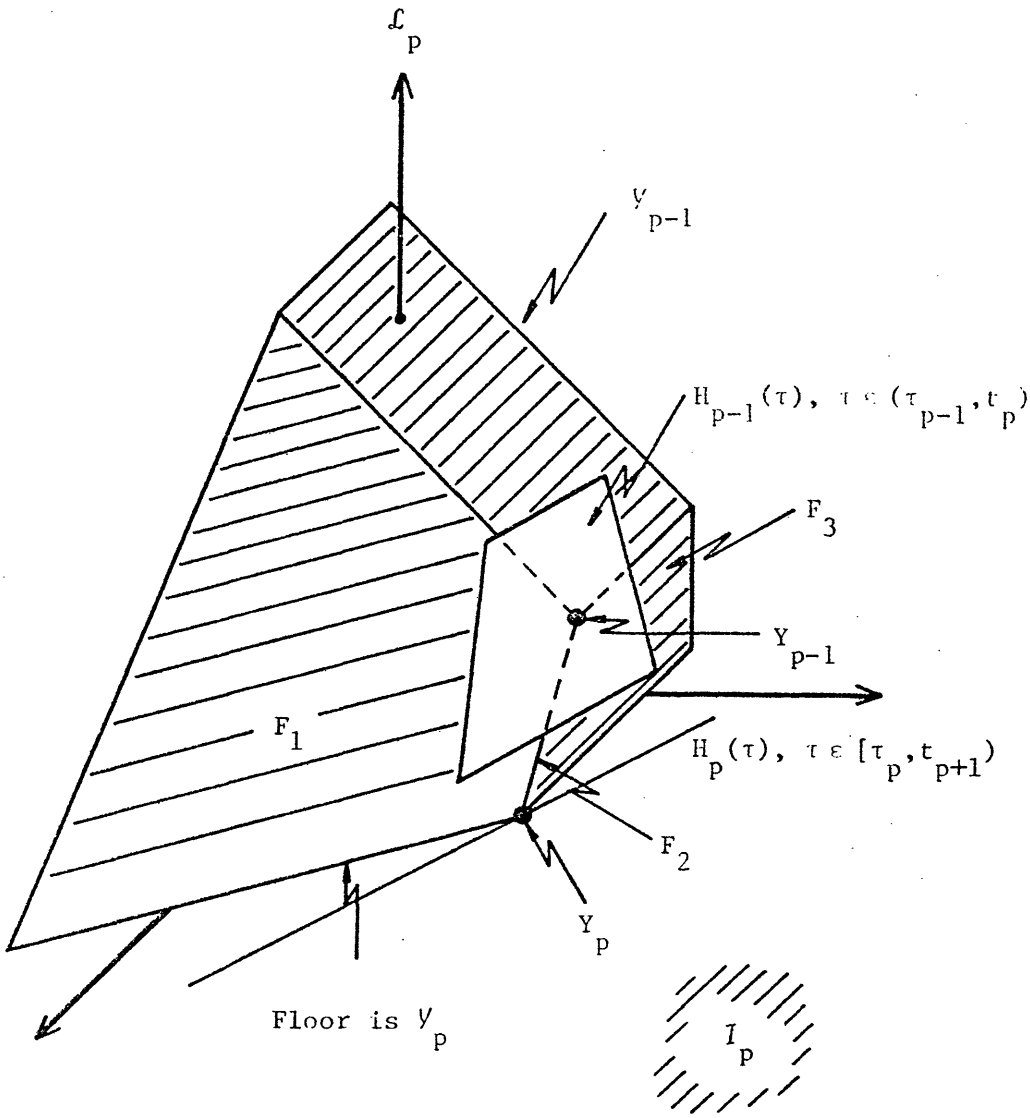

Figure 2 - Geometry in y-space associated with successive constrained optimization problems.

vertices of Y_p and all the points which are convex combinations of these vertices.

As time runs backward, the costates (coefficients) $\lambda_i^j(\tau)$ for all i,j such that $x_i^j \in I_p$ evolve according to

$$-\dot{\lambda}_i^j(\tau) = \alpha_i^j \tag{9}$$

where α_i^j is the coefficient of x_i^j in the cost functional (see eqs. (5) and (34) of [1]). The evolution of the costates in time will in general cause rotation of $H_p(\tau)$ and hence change its orientation with respect to Y_p. If $H_p(\tau)$ rotates a sufficient amount, then the surface of tangency between it and Y_p will change at the switch time τ_p. Another switch in the face of tangency occurs at τ_{p-2} and this process continues until finally the solution set $Y_{-\infty}$ is encountered at τ_{p-q+1}. $Y_{-\infty}$ remains the surface of tangency as time runs to minus infinity.

We have now completed the description of the constrained optimization problem associated with the set of state variables $\mathcal{L}_{p+1}$ leaving the boundary at t_{p+1}. To describe the succeeding step, we now allow the set of state variable $\mathcal{L}_p \subset \mathcal{B}_p$ to leave the boundary backward in time at the boundary junction time $t_p \in (-\infty, t_{p+1})$. See Figure 1, in which case we have pictured $t_p \in (\tau_p, t_{p+1})$ for convenience.[1] The constrained optimization problem in R^m corresponding to this case is

$$\underline{u}^*(\tau) = \text{ARG} \underset{\underline{u}(\tau)\in U}{\text{MIN}} \sum_{x_i^j \in I_{p-1}} \lambda_i^j(\tau)\dot{x}_i^j(\tau) , \tag{10}$$

---

1. Note that the Constructive Dynamic Programming Algorithm of Section VI of [1] calls for steps to be performed with $\mathcal{L}_p$ leaving at times within *each* of the segments $(-\infty,\tau_{p-q+1}),\ldots,[\tau_{p-1},\tau_p),[\tau_p,t_{p+1})$ corresponding to the feedback control regions $R_{p-q+1},\ldots,R_{p-1},R_p$.

subject to

$$\dot{x}_i^j(\tau) = 0 \quad \forall i,j \text{ s.t. } x_i^j \in \mathcal{B}_{p-1} \qquad (11)$$

$$\tau \in (-\infty, t_p) \quad ,$$

where $\mathcal{I}_{p-1}$ and $\mathcal{B}_{p-1}$ denote respectively the sets of state variables which are on interior arcs and boundary arcs for $\tau \in (-\infty, t_p)$. In the fashion of the previous step, the linear program (10) - (11) in R^m may be expressed as a linear program in the space whose coordinate axes are y_i^j for all i,j such that $x_i^j \in \mathcal{I}_{p-1}$, that is $R^{\sigma_p+\rho_p}$, where ρ_p is the cardinality of $\mathcal{L}_p$.

Definition 4. The $\sigma_p + \rho_p$ *dimensional constraint figure* is

$$\mathcal{Y}_{p-1} \triangleq \left\{ \underline{y} \in R^{\sigma_p+\rho_p} \,/\, \underline{y} \in \mathcal{Y} \quad \text{and} \quad y_i^j = 0 \ \forall i,j \text{ s.t. } x_i^j \in \mathcal{B}_{p-1} \right\} \quad .$$

It is readily seen that $\mathcal{Y}_{p-1}$ is a bounded convex polyhedron, and that

$$\mathcal{Y}_{p-1} = \mathcal{Y} \cap R^{\sigma_p+\rho_p} \quad , \qquad (12)$$

where $\mathcal{Y}$ is the global constraint figure of Definition 2. The constrained optimization problem of dimension $\sigma_p + \rho_p$ in y-space is

$$\underline{y}^*(\tau) = \text{ARG} \max_{\underline{y}(\tau) \in \mathcal{Y}_{p-1}} \sum_{x_i^j \in \mathcal{I}_{p-1}} \lambda_i^j(\tau) y_i^j(\tau) \qquad (13)$$

$$\tau \in (-\infty, t_p) \quad .$$

Suppose we are given a particular set of values of $\lambda_i^j(t_p)$ for all i,j such that $x_i^j \in \mathcal{I}_{p-1}$. We denote by q the number of switches which occur in the solution on $\tau \in (-\infty, t_p)$ and denote the times at which these switches occur by $\tau_{p-q}, \ldots, \tau_{p-2}, \tau_{p-1}$, where the solution remains unchanged from τ_{p-q} to minus infinity.[1] The sequence of solution sets

1. In order to avoid unnecessarily cumbersome indexing, we have used the symbols q and $\tau_{p-q+1}, \ldots, \tau_{p-1}$ both here and in the previous step. The appropriate usage shall be clear from the text. We shall also take similar liberties when referring to solution sets (Y's), optimal control

which occur on this time partition is denoted $Y_{-\infty}, Y_{p-q}, \ldots, Y_{p-2}, Y_{p-1}$ where Y_{p-1} applies on $[\tau_{p-1}, t_p)$, Y_{p-2} applies on $[\tau_{p-2}, \tau_{p-1}), \ldots,$ $Y_{-\infty}$ applies on $(-\infty, \tau_{p+q})$. $Y_{-\infty}, Y_{p-q}, \ldots, Y_{p-2}, Y_{p-1}$ are the respective images of the optimal control sets $\Omega_{-\infty}, \Omega_{p-q}, \ldots, \Omega_{p-2}, \Omega_{p-1}$, where $\Omega_{p-q}, \ldots, \Omega_{p-2}, \Omega_{p-1}$ are associated with the "break feedback control regions" $R_{p-q}, \ldots, R_{p-2}, R_{p-1}$ respectively, and $\Omega_{-\infty}$ is associated with the "non-break feedback control region" $R_{-\infty}$. In general, we shall refer to members of these y-space solution sets as $\sigma_p + \rho_p$ *dimensional operating points*.

We now proceed to the geometrical interpretation of (13). For every $\tau \in (-\infty, t_p)$ we represent the maximand of (12) as the $\sigma_p + \rho_p - 1$ *dimensional Hamiltonian hyperplane* in $R^{\sigma_p + \rho_p}$:

$$H_{p-1}(\tau): \qquad Z = \sum_{x_i^j \in I_{p-1}} \lambda_i^j(\tau) y_i^j \qquad (14)$$

The initial solution set Y_{p-1} of the linear program backward in time consists of all points of tangency between Y_{p-1} and $H_{p-1}(\tau)$ on $\tau \in [\tau_{p-1}, t_p)$. See Figure 2. As time runs backward, the costates (coefficients) $\lambda_i^j(\tau)$, for all i,j such that $x_i^j \in I_{p-1}$, evolve according to (9) causing the rotation of $H_{p-1}(\tau)$. This causes the solution set to switch successively from Y_{p-1} to Y_{p-2} at τ_{p-1}, Y_{p-2} to Y_{p-3} at $\tau_{p-2}, \ldots, Y_{p-q}$ to $Y_{-\infty}$ at τ_{p-q}. $Y_{-\infty}$ persists until time equals minus infinity.

We have now described in geometrical terms the nature of the constrained optimization problems corresponding to successive steps of the Constructive Dynamic Programming Algorithm. In summary, when we allow state variables to leave the boundary backward in time, we enlarge the space of decision variables in y-space by releasing constraints of the form $y_i^j = 0$. As the constraint figure grows in dimension (from the σ_p dimensional Y_p

to the $\sigma_p + \rho_p$ dimensional Y_{p-1}), so also do the associated Hamiltonian hyperplanes (from the $\sigma_p - 1$ dimensional H_p to the $\sigma_p + \rho_p - 1$ dimensional H_{p-1}).

C. Geometrical Relationship Between Successive Constrained Optimization Problems

Let us return to the point in the description above in which we allow the set of state variables $\mathcal{L}_p$ to leave the boundary backward in time at some $t_p \in (-\infty, t_{p+1})$. *For convenience in this and subsequent discussions, we consider the case in which* $t_p \in [\tau_p, t_{p+1})$ *as depicted in Figure 1. This corresponds to* $\mathcal{L}_p$ *leaving the feedback control region* R_p. This discussion could apply equally well to any of the other cases $t_p \in [\tau_{p-1}, \tau_p), \ldots, t_p \in (-\infty, \tau_{p-q+1})$ with an appropriate change of notation.

We now consider the constrained optimization problems which occur at t_p^- and t_p^+, the times immediately before and after t_p, respectively, in the backward sense of time. Summarizing the notation of Section III.B, we have

at t_p^-, (t_p^+):

- $B_p, (B_{p-1})$ - set of state variables on boundary arcs
- $I_p, (I_{p-1})$ - set of state variables on interior arcs
- $\sigma_p, (\sigma_p + \rho_p)$ - dimension of constrained optimization problem in y-space, i.e., cardinality of $I_p, (I_{p-1})$
- $Y_p, (Y_{p-1})$ - constraint figure in y-space
- $H_p, (H_{p-1})$ - Hamiltonian hyperplane
- $Y_p, (Y_{p-1})$ - solution set in y-space
- $R_p, (R_{p-1})$ - feedback control region corresponding to $[\tau_p, t_{p+1})$, $([\tau_{p-1}, t_p))$

at t_p: $\mathcal{L}_p$ - set of state variables leaving boundary

ρ_p - cardinality of $\mathcal{L}_p$.

We begin by noting that (6) and (12) together imply

$$Y_p = Y_{p-1} \bigcap R^{\sigma_p} \quad , \tag{15}$$

that is, Y_p is the projection of Y_{p-1} onto R^{σ_p}. Therefore, all boundary points of Y_p are also boundary points of Y_{p-1}.

Let R^{ρ_p} be the space whose coordinate axes are y_i^j for all i,j such that $x_i^j \in \mathcal{L}_p$. Then by Definition 1 any point in the positive orthant of R^{ρ_p} corresponds to having $\dot{x}_i^j$ strictly negative (in forward time) for all $x_i^j \in \mathcal{L}_p$. Since we call for all state variables $x_i^j \in \mathcal{L}_p$ to leave the boundary backward in time at t_p, then Y_{p-1} must contain *at least one point* in the positive orthant of R^{ρ_p}. This argument motivates the following definition:

Definition 5. An *$\mathcal{L}_p$-positive face of Y_{p-1} with respect to Y_p* is any face of Y_{p-1} which contains Y_p and also at least one point in the positive orthant of R^{ρ_p}.

The notation of Definition 5 is illustrated in Figure 2, where F_1, F_2 and F_3 are $\mathcal{L}_p$-positive faces of Y_{p-1} with respect to Y_p.

The following theorem is a geometrical consequence of the necessary condition that stipulates continuity of the Hamiltonian function.

Theorem 1

(a) $H_p(t_p) = H_{p-1}(t_p) \bigcap R^{\sigma_p}$

(b) $H_{p-1}(t_p)$ contains an $\mathcal{L}_p$-positive face of Y_{p-1} with respect to Y_p.

Proof:

(a) The Hamiltonian hyperplane H_p at t_p^- is

$$H_p(t_p^-): \quad Z^- = \sum_{x_i^j \varepsilon I_p} \lambda_i^j(t_p^-) y_i^j \quad , \tag{16}$$

and the Hamiltonian hyperplane H_{p-1} at t_p^+ is

$$H_{p-1}(t_p^+): \quad Z^+ = \sum_{x_i^j \varepsilon I_p} \lambda_i^j(t_p^+) y_i^j + \sum_{x_i^j \varepsilon \mathcal{L}_p} \lambda_i^j(t_p^+) y_i^j \quad . \tag{17}$$

Now, $Y_p \subset H_p(t_p^-)$ and $Y_{p-1} \subset H_{p-1}(t_p^+)$ according to the geometric interpretation. If we now evaluate $H_p(t_p^-)$ at any point in Y_p and $H_{p-1}(t_p^+)$ at any point in Y_{p-1}, the continuity of the Hamiltonian everywhere (equation (2) of [1]) gives

$$Z^+ = Z^- = Z^* \quad . \tag{18}$$

Furthermore, the continuous nature of costates corresponding to state variables on interior arcs (equation (34) of [1]) gives

$$\lambda_i^j(t_p^-) = \lambda_i^j(t_p^+) = \lambda_i^j(t_p) \quad \forall i,j \text{ s.t. } x_i^j \varepsilon I_p \quad . \tag{19}$$

By virtue of (18) and (19), we may write the Hamiltonian hyperplanes

$$H_p(t_p): \quad Z^* = \sum_{x_i^j \varepsilon I_p} \lambda_i^j(t_p) y_i^j \tag{20}$$

$$H_{p-1}(t_p): \quad Z^* = \sum_{x_i^j \varepsilon I_p} \lambda_i^j(t_p) y_i^j + \sum_{x_i^j \varepsilon \mathcal{L}_p} \lambda_i^j(t_p^+) y_i^j \quad . \tag{21}$$

We conclude immediately from (20) and (21) that $H_p(t_p) = H_{p-1}(t_p) \bigcap R^{\sigma_p}$.

(b) The argument preceding Definition 5 concludes that Y_{p-1} must contain at least one point in the positive orthant of R^{ρ_p}, say $\underline{y}_{p-1}$; therefore $\underline{y}_{p-1}$ is contained in $H_{p-1}(t_p)$. From statement (a) of the theorem we have that $H_{p-1}(t_p)$ contains $H_p(t_p)$ and therefore contains Y_p. Consequently, $H_{p-1}(t_p)$ must contain the $\mathcal{L}_p$-positive face which contains both Y_p and $\underline{y}_{p-1}$.

□ Theorem 1

The geometry associated with Theorem 1 is depicted in Figure 3.

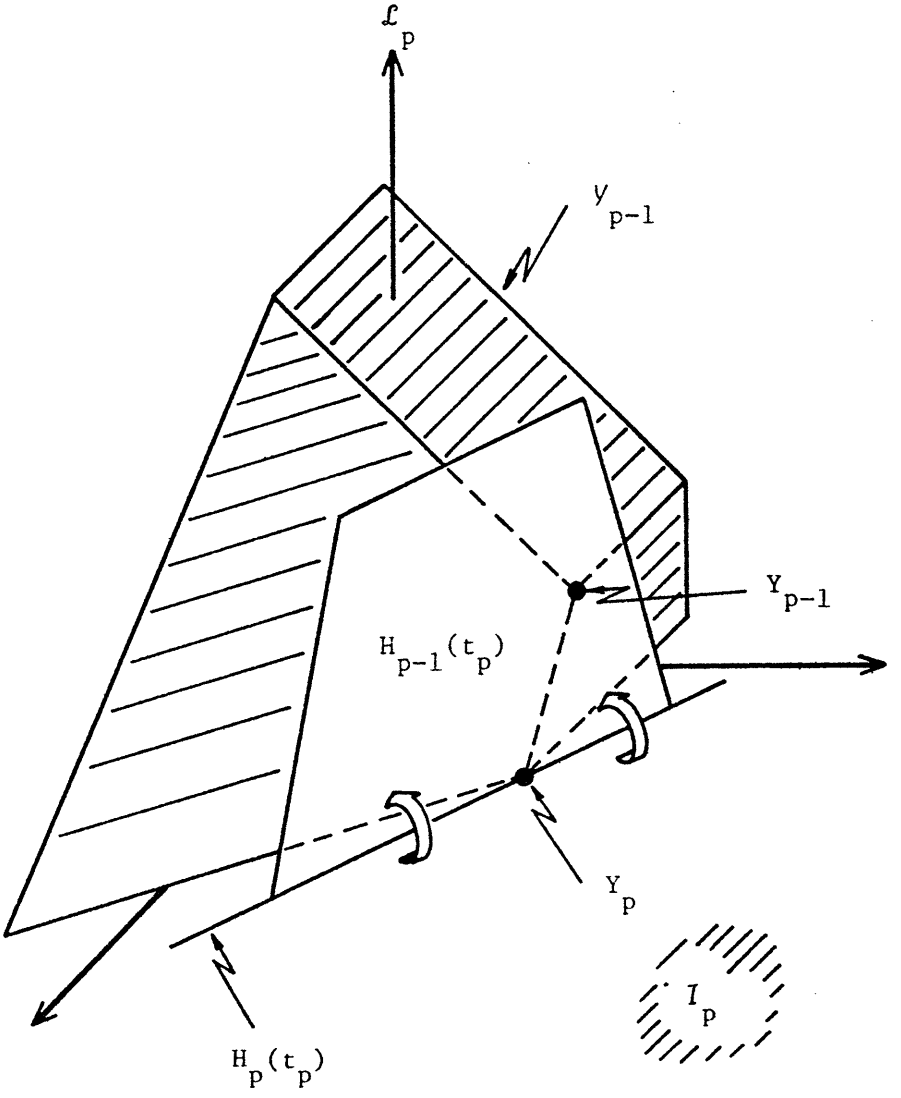

Figure 3 - Geometry associated with Theorem 1.

III. PROBLEMS OF THE CONSTRUCTIVE DYNAMIC PROGRAMMING ALGORITHM

The four problems associated with the Constructive Dynamic Programming are now discussed in the light of the geometrical interpretation developed in the previous section. The order of the presentation of the problems differs from that in which they appear in the description of the algorithm in Section VI of [1]. In each instance, we first present a brief statement of the issue as it relates to the algorithm, and afterwards provide the appropriate geometrical interpretation. The reader is reminded that attention is being focused on the case in which $t_p \in (\tau_p, t_{p+1})$, as discussed in Section II-C.

A. Leave-the-Boundary Costates

Operation 2 of the algorithm calls for finding those values of the costate vector at t_p which satisfy the necessary conditions and allow for the optimal departure of $\mathcal{L}_p$ from the boundary backward in time *or* for showing that no such values exist. In detail, given specific values of $\lambda_i^j(t_p)$, all i,j such that $x_i^j \in I_p$, we must find those values of $\lambda_i^j(t_p)$, all i,j such that $x_i^j \in \mathcal{L}_p$, so that when maximizing $H_{p-1}(t_p)$ over Y_{p-1} the solution has $\dot{x}_i^j < 0$ for all $x_i^j \in \mathcal{L}_p$, *or* we must show that no such values of $\lambda_i^j(t_p)$ exist.

Geometrically, Theorem 1 says that we essentially want to rotate $H_{p-1}(t_p)$ *around* $H_p(t_p)$ *by increasing from zero the coefficients* $\lambda_i^j(t_p)$, *all* i,j *such that* $x_i^j \in \mathcal{L}_p$, *until* $H_{p-1}(t_p)$ *touches* Y_{p-1} *on an* $\mathcal{L}_p$*-positive face with respect to* Y_p. *The values of these coefficients at which this condition is achieved constitute a particular set of leave-the-boundary costates at* t_p *provided that they are among the globally optimizing values*

for the previous step.[1]

The rotation is depicted by the arrows in Figure 3. Note that the rotation is performed while holding time fixed at t_p ($\lambda_i^j(t_p)$ for all i,j such that $x_i^j \varepsilon I_p$ do not change) and is to be distinguished from the rotation of the Hamiltonian hyperplane which results from the costates evolving backward in time.

Suppose that there is more than one such $\mathcal{L}_p$-positive face (of various dimensions $\leq \sigma_p + \rho_p - 1$) to which $H_{p-1}(t_p)$ may be rotated in the above fashion. Then the leave-the-boundary costates achieve those values which bring $H_{p-1}(t_p)$ to lie on each of these faces (this is a finitely non-unique set) *and* those values which have $H_{p-1}(t_p)$ lying everywhere between these faces (this is an infinitely non-unique set). However, the algorithm requires only extreme operating points of Y_{p-1}, that is vertices of Y_{p-1}, for constructing feedback control regions (Operation 4, Section VI of [1]). Hamiltonian hyperplanes which lie between faces of Y_{p-1} provide no extreme operating points in addition to those which lie on the faces. Hence, *the leave-the-boundary costate set at* t_p *can be taken as that finite set corresponding to each of the highest dimensional* $\mathcal{L}_p$*-positive faces upon which* $H_{p-1}(t_p)$ *may be made to lie.* See Example 1 of Section IV.

Finally, it may be that there are no appropriate values of $\lambda_i^j(t_p)$, all i,j such that $x_i^j \varepsilon \mathcal{L}_p$, which allow $H_{p-1}(t_p)$ to lie on an $\mathcal{L}_p$-positive face with respect to Y_p. In that case it is *not* optimal for $\mathcal{L}_p$ to leave the boundary backward in time at t_p.

---

1. The specification of the globally optimizing values for *this step* is provided in Section III-C. This explanation is easily framed in terms of the previous step as required here.

B. Subregions

Operation 1 of the algorithm calls for partitioning the feedback control region R_p into subregions with respect to $\mathcal{L}_p$. A subregion $R_p(\mathcal{L}_p)$ of R_p is the set of all those points in R_p which when taken as the point of departure of $\mathcal{L}_p$ result in a common Ω and W. Here $\Omega = \{\Omega_{-\infty}, \Omega_{p-q}, \ldots, \Omega_{p-2}, \Omega_{p-1}\}$ is the collection of optimal control sets and $W = \{w_{p-q}, \ldots, w_{p-2}, w_{p-1}\}$ is the collection of breakwalls encountered on $(-\infty, t_p)$ for a particular $t_p \in (\tau_p, t_{p+1})$. See Operation 3, Section VI of [1]. If there are s subregions in a particular partition, then the subregions are denoted as $R_p^1(\mathcal{L}_p), R_p^2(\mathcal{L}_p), \ldots, R_p^{s-1}(\mathcal{L}_p), R_p^s(\mathcal{L}_p)$.

The *geometrical interpretation* for determining subregions in general is not currently understood. In order to get some basic idea of what is involved, we consider here the simplifying situation in which the control does not break on $(-\infty, t_p)$; that is, there are no breakwalls with which to be concerned. In this case, a subregion $R_p(\mathcal{L}_p)$ of R_p is simply the set of all those points in R_p which when taken as the point of departure of $\mathcal{L}_p$ result in a common $\Omega_{-\infty}$, or from the geometrical point of view, a common $Y_{-\infty}$.

For illustration we consider the portion of a *particular* optimal trajectory which lies in R_p and occurs on the time interval $[\tau_p, t_{p+1})$. This is depicted by the heavy line in Figure 4. The y-space operating point corresponding to this trajectory portion is Y_p. We now observe what happens as we allow the boundary junction time for $\mathcal{L}_p$, that is t_p, vary from t_{p+1} to τ_p - this is equivalent to allowing the point of departure of $\mathcal{L}_p$ from R_p vary along the line joining $\underline{x}(t_{p+1})$ and $\underline{x}(\tau_p)$.

Let us start by taking $t_p = t_{p+1}$. According to Theorem 1, $Y_{-\infty}$ will then consist of points which lie on the $\mathcal{L}_p$-positive face of Y_{p-1} with

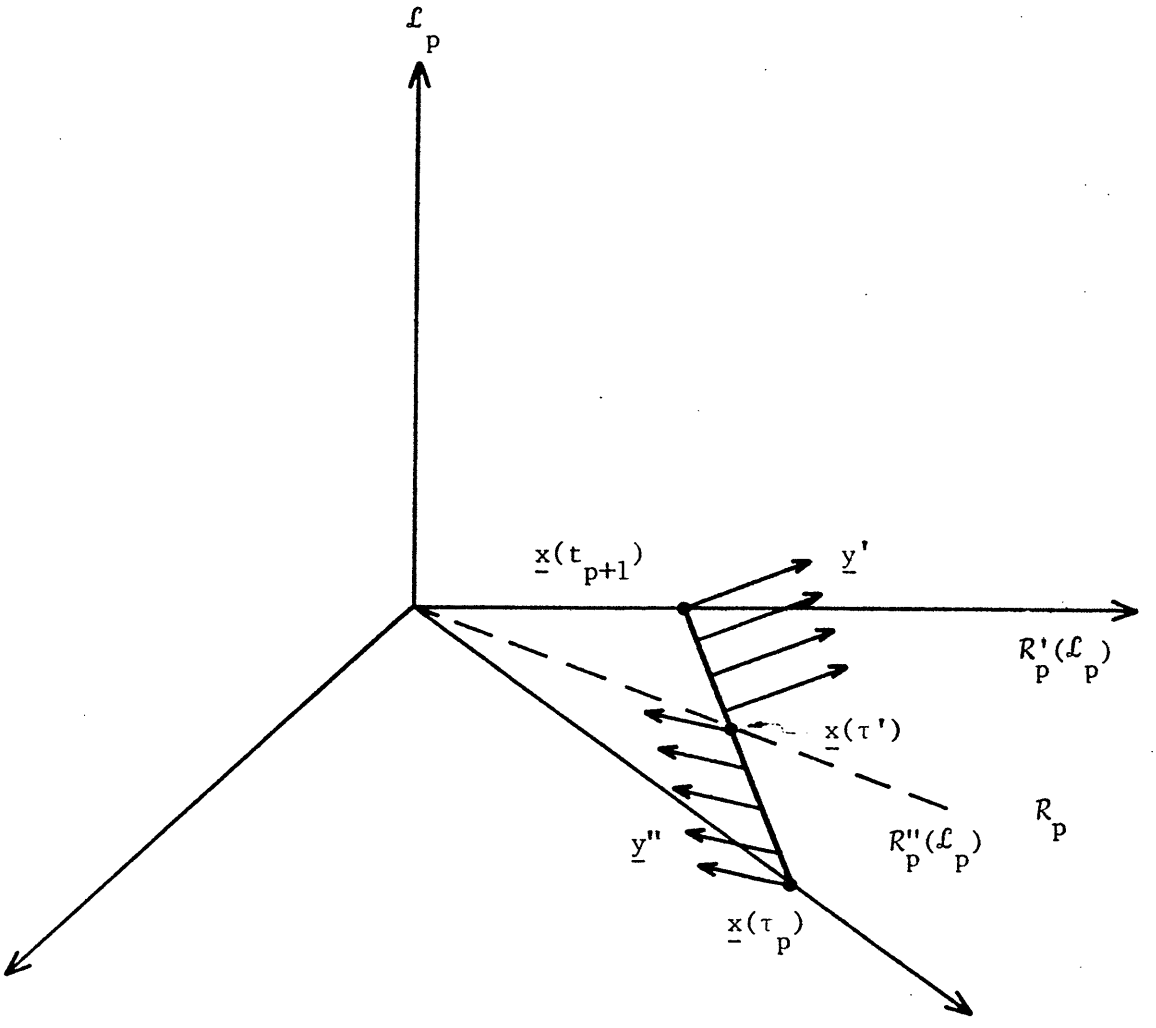

Figure 4 - Illustration of subregions of R_p with respect to $\mathcal{L}_p$.

respect to Y_p to which $H_{p-1}(t_p)$ may be rotated around $H_p(t_p)$ at $t_p = t_{p+1}$. For the sake of simplicity we shall assume that $Y_{-\infty}$ consists of exactly one point $\underline{y}'$. The corresponding direction in which $\mathcal{L}_p$ leaves R_p at $t_p = t_{p+1}$ is indicated by the arrow emanating from the point $\underline{x}(t_{p+1})$ in Figure 4.

Now, as t_p assumes values continuously backward from t_{p+1} the solution set $Y_{-\infty} = \underline{y}'$ persists until some time $t_p = \tau'$. *At this time the set* $Y_{-\infty}$ *will change due to the fact that the* $\mathcal{L}_p$*-positive face of* Y_{p-1} *with respect to* Y_p *upon which* $H_{p-1}(t_p)$ *may be made to lie changes. This is attributable to the fact that* $H_p(t_p)$ *is rotating as* $\lambda_i^j(t_p)$, *all* i,j *such that* $x_i^j \in I_p$, *evolve backward in time.* Once again, for simplicity, assume that the new value of $Y_{-\infty}$ is unique and denote it by $\underline{y}''$. The corresponding direction with which $\mathcal{L}_p$ leaves R_p at $t_p = \tau'$ is indicated by the arrow emanating from the point $\underline{x}(\tau')$ in Figure 4.

Assume that the solution set $Y_{-\infty} = \underline{y}''$ persists from τ' to τ_p. Then in this particular situation R_p consists of two subregions with respect to $\mathcal{L}_p$, $R_p'(\mathcal{L}_p)$ and $R_p''(\mathcal{L}_p)$ as indicated in Figure 4. The point $\underline{x}(\tau')$ lies on a wall separating $R_p'(\mathcal{L}_p)$ and $R_p''(\mathcal{L}_p)$.

Knowledge of $\underline{x}(\tau')$ alone is sufficient to determine this wall *only for the case in which* R_p *is two dimensional* - see Example 2 of Section IV for an illustration of this. For R_p of arbitrarily high dimension it is clear that some correspondingly high number of trajectories lying in R_p must be considered from the above point of view, although it is not currently understood how this may be achieved. Also, since the above discussion is predicated upon special simplifying assumptions concerning Ω, W and Y, our knowledge concerning the very difficult problem of determining subregions in general is quite incomplete.

C. Global Optimality

Operation 3 of the algorithm for the step under discussion calls for finding all solutions to the global optimization problem on $\tau \in (-\infty, t_p)$ which satisfy the constraints $\dot{x}_i^j(\tau) = 0$ for all i,j such that $x_i^j \in \mathcal{B}_{p-1}$ *or* show that no such solution exists. In Appendix A of [1] a two-part approach is suggested for solving this problem:

(a) Find all solutions to the constrained optimization problem.

(b) Produce values of $\lambda_i^j(\tau)$, all i,j such that $x_i^j \in \mathcal{B}_{p-1}$, and all $\tau \in (-\infty, t_p)$, which satisfy the necessary conditions (15) - (17) of [1], and such that all solutions to part (a) are also solutions to the global optimization problem (1) *or* show that no such values exist.

As a complete discussion of part (a) is provided in Appendix A of [1], we concern ourselves here with the solution of part (b).

We begin by specifying those values of $\lambda_i^j(\tau)$, all i,j such that $x_i^j \in \mathcal{B}_{p-1}$ and all $\tau \in (-\infty, t_p)$ which satisfy the necessary conditions. According to equations (15) - (17) of [1], the appropriate costate differential equations are:

$$-d\lambda_i^j(\tau) = \alpha_i^j d\tau + d\eta_i^j(\tau) \tag{22}$$

$$d\eta_i^j(\tau) \leq 0 \tag{23}$$

$$\forall i,j \text{ s.t. } x_i^j \in \mathcal{B}_{p-1}, \quad \tau \in (-\infty, t_p) \quad .$$

If we take τ to be time running backward from t_p, then equations (22) - (23) indicate that the maximum value that any $\lambda_i^j(\tau)$, i,j such that $x_i^j \in \mathcal{B}_{p-1}$, may achieve *for a given* $\lambda_i^j(t_p)$ is when $d\eta_i^j(\tau) = 0$. Therefore

$$\lambda_i^j(\tau) \leq \lambda_i^j(t_p) + \tau\alpha_i^j \qquad (24)$$

$$\forall\, i,j \text{ such that } x_i^j \in B_{p-1} .$$

We now provide the *geometrical interpretation* of part (b), the test for global optimality of the constrained solution on $(-\infty,t_p)$. First, the $\underline{u}$-space constrained solution sets $\Omega_{-\infty},\Omega_{p-q},\ldots,\Omega_{p-2},\Omega_{p-1}$ are globally optimal if and only if the corresponding $\underline{y}$-space constrained solution sets $Y_{-\infty},Y_{p-q},\ldots,Y_{p-2},Y_{p-1}$ are globally optimal. We consider the latter sets one at a time beginning with Y_{p-1}.

According to the geometrical interpretation of the constrained optimization problem (Section II-B), Y_{p-1} is the surface of tangency between the Hamiltonian hyperplane $H_{p-1}(\tau)$ of equation (20) and the constraint figure $\mathcal{Y}_{p-1}$. In accordance with the geometrical interpretation of the global optimization problem (Section II-A), Y_{p-1} is a global optimum if and only if there exist values of $\lambda_i^j(\tau)$, all i,j such that $x_i^j \varepsilon B_{p-1}$ and all $\tau \varepsilon [\tau_{p-1},t_p)$, which satisfy the necessary conditions and such that the global Hamiltonian hyperplane $H(\tau)$ of (3) is tangent to the global constraint figure $\mathcal{Y}$ at Y_{p-1}. The preceding condition holds true for all $\tau \varepsilon [\tau_{p-1},t_p)$ if and only if it holds true for any $\tau \varepsilon [\tau_{p-1},t_p)$. These observations suggest the following test for global optimality of Y_{p-1}:

Choose any $\tau \varepsilon [\tau_{p-1},t_p)$. *Then* Y_{p-1} *is a global optimum if and only if there exist values of* $\lambda_i^j(\tau)$ *for all* i,j *such that* $x_i^j \varepsilon B_{p-1}$ *which satisfy the necessary conditions and which cause* $H(\tau)$ *to rotate about* $H_{p-1}(\tau)$ *until* $H(\tau)$ *becomes tangent to* $\mathcal{Y}$ *at* Y_{p-1}.

All values of $\lambda_i^j(\tau)$, i,j such that $x_i^j \varepsilon B_{p-1}$, which satisfy the above condition constitute the *globally optimizing* set at τ. This test is illustrated for

a simple situation in Example 3 of Section IV. If Y_{p-1} is found not to be a globally optimizing solution, then it is *not* optimal for the state variables in $\mathcal{L}_p$ to leave the boundary. If Y_{p-1} is a global optimum, we next test Y_{p-2} and continue in this fashion until some constrained solution is shown not to be globally optimum or $Y_{-\infty}$ is reached. Feedback control regions are constructed corresponding to all globally optimal solutions.

D. Off-the-Boundary Assumption

Preceding the description of a step of the algorithm in Section VI of [1], the following assumption is made, which we call the *off-the-boundary assumption: it is optimal for all of the state variables in* I_{p-1} *to remain off the boundary as time runs to minus infinity.* This assumption is implicit in the structure of the Constructive Dynamic Programming Algorithm since each state variable is allowed to leave the boundary backward in time exactly once for each optimal trajectory constructed. In principle, the algorithm can be formulated in the absence of this assumption, but it then becomes extremely complex.

We now provide the rather simple *geometrical interpretation* associated with this assumption:

The off-the-boundary assumption is true for the current step if and only if there exist constrained solution sets $Y_{-\infty}, Y_{p-q}, \ldots, Y_{p-2}, Y_{p-1}$ *which all lie in the non-negative orthant of* $R^{\sigma_p+\rho_p}$ *and all of which are global optima.*

This geometrical interpretation is illustrated in Example 4 of Section IV.

IV. ILLUSTRATIONS OF THE GEOMETRICAL INTERPRETATION

A. Leave-the-Boundary Costates

Example 1 demonstrates the geometrical interpretation for determining the leave-the-boundary costates for a situation in which these costates are non-unique.

Example 1

The general network topology to be considered in this and several other examples is depicted in Figure 5. The link capacities are indicated in brackets, and for simplicity the inputs are all taken to be zero. The equations of motion are

$$\begin{aligned}
\dot{x}_1^2(t) &= -u_{12}^2(t) - u_{13}^2(t) + u_{31}^2(t) \\
\dot{x}_2^1(t) &= -u_{21}^1(t) - u_{23}^1(t) + u_{32}^1(t) \\
\dot{x}_1^3(t) &= -u_{13}^3(t) - u_{12}^3(t) + u_{21}^3(t) \\
\dot{x}_3^1(t) &= -u_{31}^1(t) - u_{32}^1(t) + u_{23}^1(t) \\
\dot{x}_2^3(t) &= -u_{23}^3(t) - u_{21}^3(t) + u_{12}^3(t) \\
\dot{x}_3^2(t) &= -u_{32}^2(t) - u_{31}^2(t) + u_{13}^2(t) \quad .
\end{aligned} \tag{25}$$

Let us limit attention now to the state variables x_3^1, x_3^2 and x_2^1 and take the cost functional to be

$$J = \int_{t_o}^{t_f} [x_3^1(t) + x_3^2(t) + x_2^1(t)]\,dt \quad . \tag{26}$$

The y-space constraint figure for this problem can readily be obtained by finding the vertices of U, transforming them into y-space via $\underline{y} = -\underline{B}\underline{u} - \underline{a}$ and finally taking the convex hull. The result is presented in Figure 6.

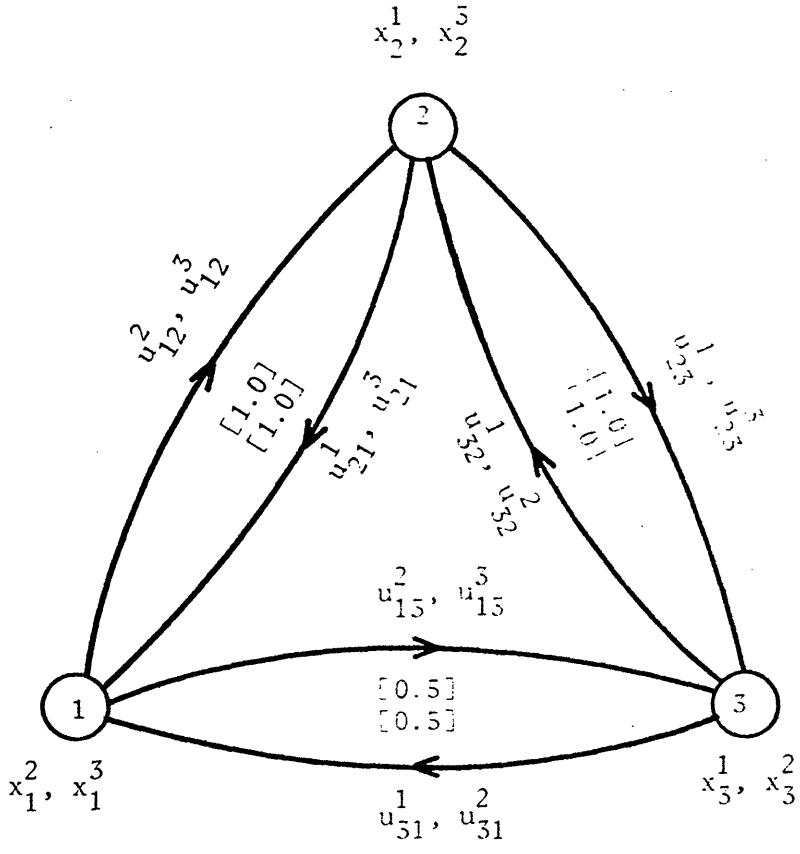

Figure 5 - Network topology for Examples 1,3 and 4.

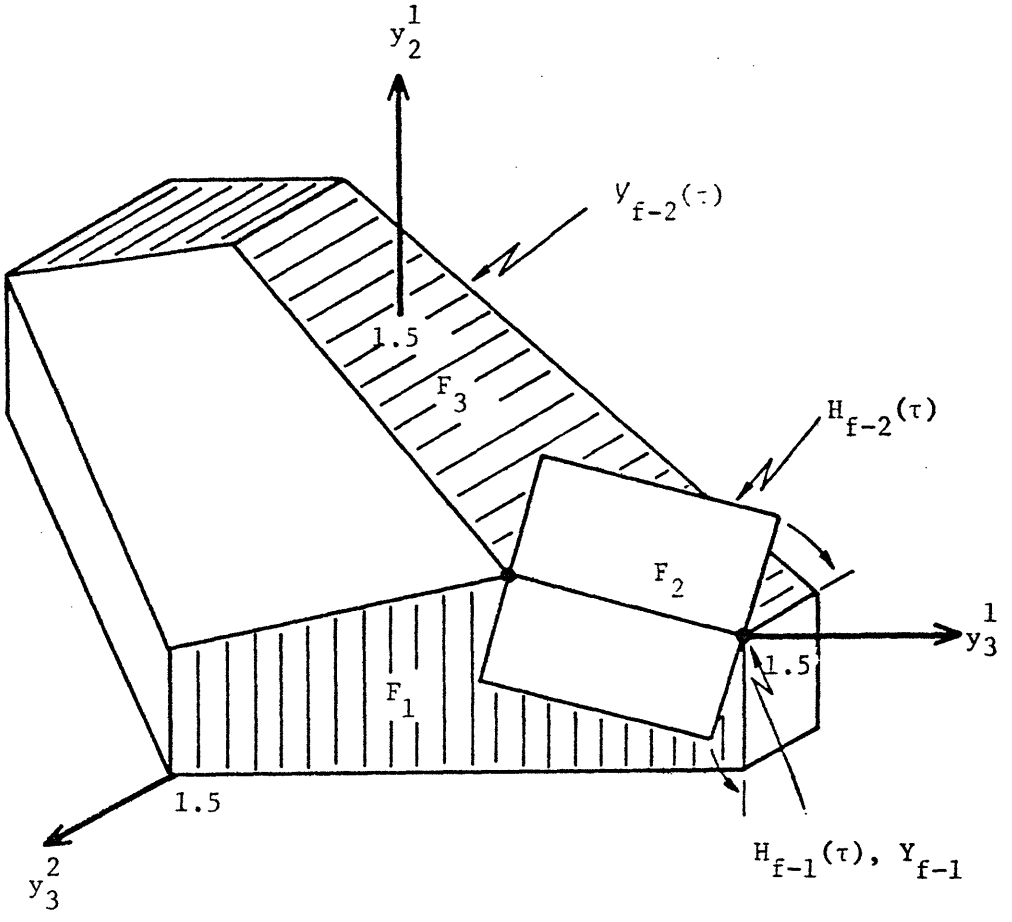

Figure 6 - Geometrical demonstration of non-uniqueness of leave-the-boundary costates.

We begin by allowing x_3^1 to leave the boundary backward in time at t_f. Since $\lambda_3^1(t_f) = 0$ (Corollary 2 of [1]), and $\dot{\lambda}_3^1(\tau) = -1$ (equation (34) of [1]), then $\lambda_3^1(\tau) > 0$ after x_3^1 leaves the boundary backward in time. Therefore, the zero dimensional Hamiltonian hyperplane $H_{f-1}(\tau)$: $Z = \lambda_3^1(\tau)y_3^1$ is minimized over $\mathcal{Y}_{f-1}$ at the point Y_{f-1}: $y_3^1 = 1.5$, $y_3^2 = y_2^1 = 0$ as depicted in Figure 6. This solution is of the non-break variety since it does not change as time approaches minus infinity as long as no other state variables leave the boundary.

We now allow x_3^2 and x_2^1 to leave the boundary *simultaneously* at some arbitrary boundary junction time $t_{f-1} \in (-\infty, t_f)$, that is, $\mathcal{L}_{f-1} = \{x_3^2, x_2^1\}$. Then according to Definition 5, the $\mathcal{L}_{f-1}$-positive faces of $\mathcal{Y}_{f-2}$ with respect to Y_{f-1} are F_1, F_2 and F_3 of Figure 6. Furthermore, the two dimensional Hamiltonian hyperplane $H_{f-2}(t_{f-1})$: $Z = \lambda_3^1(t_{f-1})Y_3^1 + \lambda_3^2(t_{f-1})y_3^2 + \lambda_2^1(t_{f-1})y_2^1$ can be rotated about the zero dimensional Hamiltonian hyperplane $H_{f-1}(t_{f-1})$ to touch $\mathcal{Y}_{f-2}$ in all the faces F_1, F_2 and F_3. In fact, it may lie on F_2 anywhere between F_1 and F_3. Therefore, the leave-the-boundary costates λ_3^2 and λ_2^1 at t_{f-1} may achieve values anywhere between

$$\begin{cases} \lambda_3^2(t_{f-1}) = \lambda_3^1(t_{f-1}) = t_f - t_{f-1} \\ \lambda_2^1(t_{f-1}) = 0 \end{cases}$$

and

$$\begin{cases} \lambda_3^2(t_{f-1}) = 0 \\ \lambda_2^1(t_{f-1}) = \lambda_3^1(t_{f-1}) = t_f - t_{f-1} \end{cases} .$$

Hence, we have an infinitely non-unique set of leave-the-boundary costates at t_{f-1}. This non-uniqueness persists even after x_3^2 and x_2^1 leave the boundary backward in time, and enter onto interior arcs.

□ Example 1.

B. Subregions

We now present an example of the geometrical interpretation applied to determining subregions. In this case there are two subregions in a particular two-dimensional feedback control region and the partition into subregions is readily performed.

Example 2

The network is pictured in Figure 7. Once again, for simplicity we are considering the no-inputs case. This is a single destination network with all messages intended for node 4; therefore, we may eliminate the destination superscript on the state and control variables. The dynamical equations are

$$\begin{aligned} \dot{x}_1(t) &= u_{21}(t) + u_{31}(t) - u_{14}(t) \\ \dot{x}_2(t) &= -u_{21}(t) \\ \dot{x}_3(t) &= -u_{31}(t) \end{aligned} \tag{26}$$

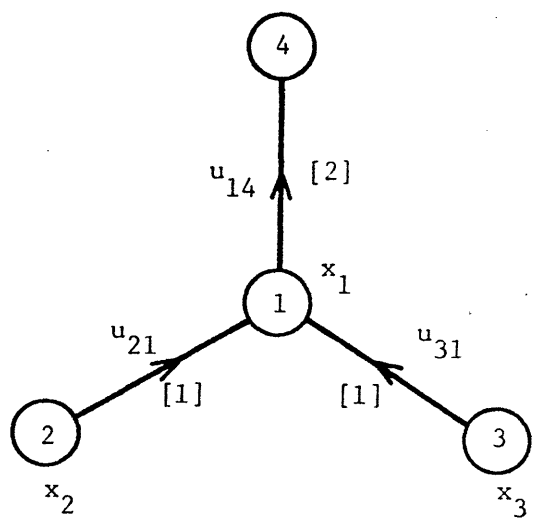

Figure 7 - Network Topology for Example 2

and we consider the cost functional

$$J = \int_{t_o}^{t_f} [2x_1(t) + x_2(t) + 2x_3(t)]dt \ . \qquad (27)$$

The y-constraint figure is depicted in Figure 8.

We begin by letting x_2 leave the boundary backward in time at t_f. The constrained optimization problem calls for the maximization of the zero dimensional Hamiltonian hyperplane $H_{f-1}(\tau)$: $Z = \lambda_2(\tau)y_2$ over the constraint figure Y_{f-1} depicted in Figure 8. The costate trajectory for λ_2 is shown in Figure 9. The solution to the constrained optimization problem is Y_{f-1}: $y_1 = 0$, $y_2 = 1.0$, $y_3 = 0$. Moreover, it is easy to see by examining Figure 8a that this solution is globally optimal for the costate values $\lambda_1(\tau) = \lambda_3(\tau) = 0$. Also, Y_{f-1} persists as time runs to minus infinity if no other state variables leave the boundary backward in time. The trajectory is illustrated in Figure 9. By a simple application of Theorem B.1 of [1], the non-break feedback control region R_{f-1} may be assigned on the x_2-axis as depicted in Figure 10.

We next stipulate that x_3 leaves the boundary at some arbitrary boundary junction time t_{f-1}. The Hamiltonian hyperplane that touches the constraint figure Y_{f-2} in the positive orthant of Y_3 is simply $H_{f-2}(t_{f-1})$: $Z = \lambda_2(t_{f-1})y_2$. Therefore, the leave-the-boundary value of λ_3 at t_f is zero. As we proceed backward in time from t_{f-1}, the one-dimensional Hamiltonian hyperplane $H_{f-2}(\tau)$: $Z = \lambda_2(\tau)y_2 + \lambda_3(\tau)y_3$ is maximized over Y_{f-2} at the point Y_{f-2}: $y_1 = 0$, $y_2 = 1.0$, $y_3 = 1.0$. This solution is globally optimal for $\lambda_1(\tau) = 0$ and does not experience a break as time runs to minus infinity if no other state variables leave the boundary backward in time. We construct the two-dimensional non-break feedback control region labled R_{f-2} in Figure 10 by once again applying Theorem B.1 of [1].

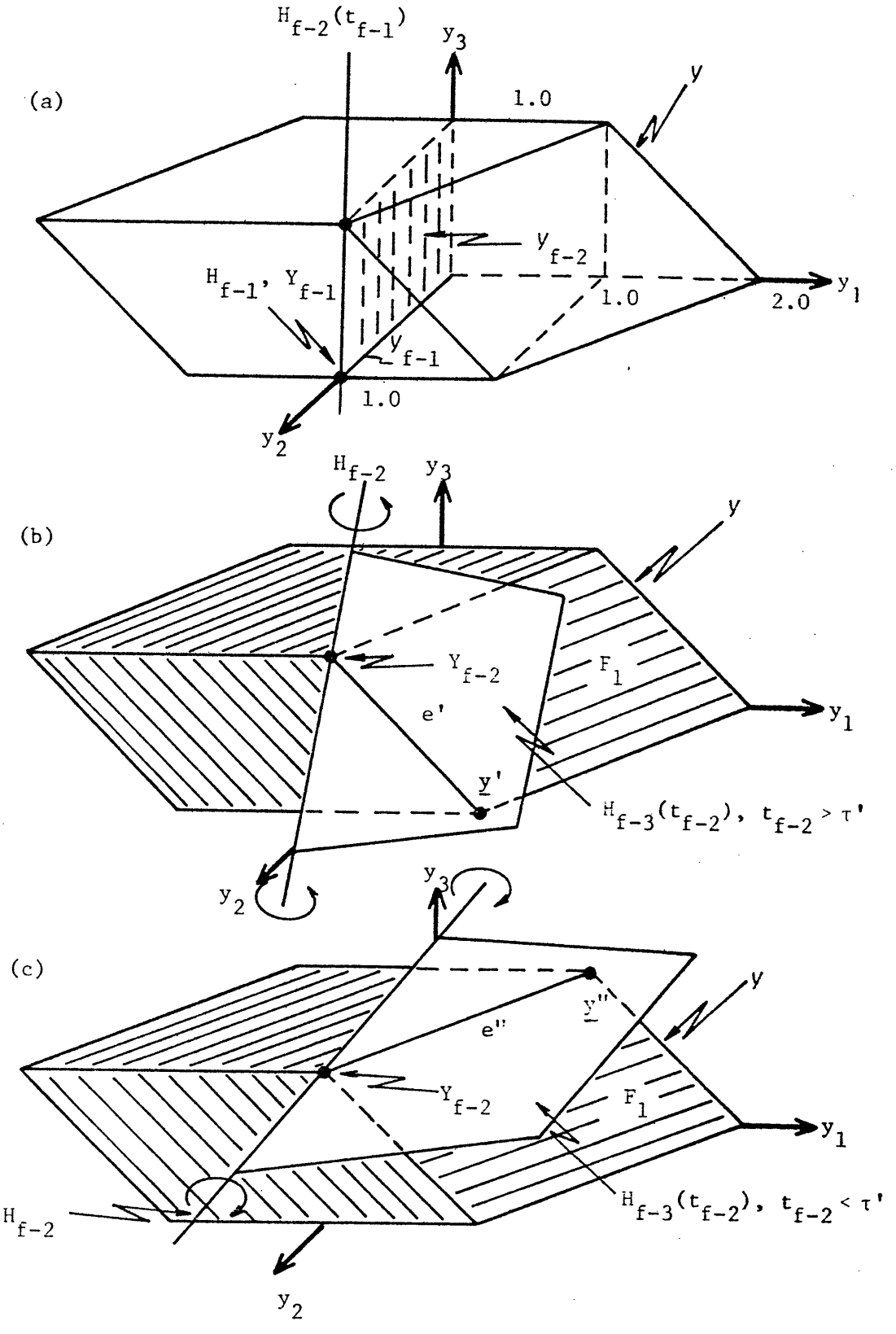

Figure 8 - Geometry for Example 2.

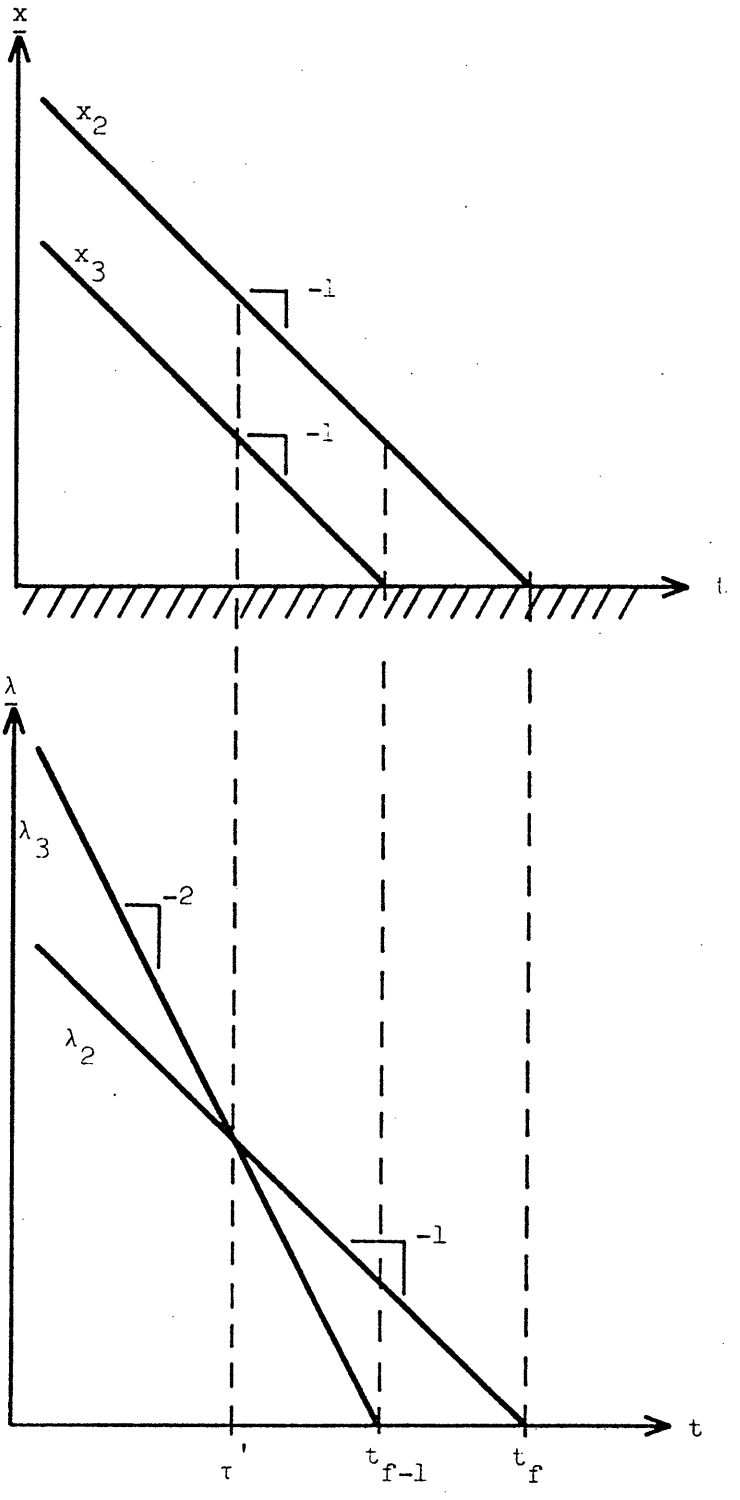

Figure 9 - State-costate trajectory pair for Example 2.

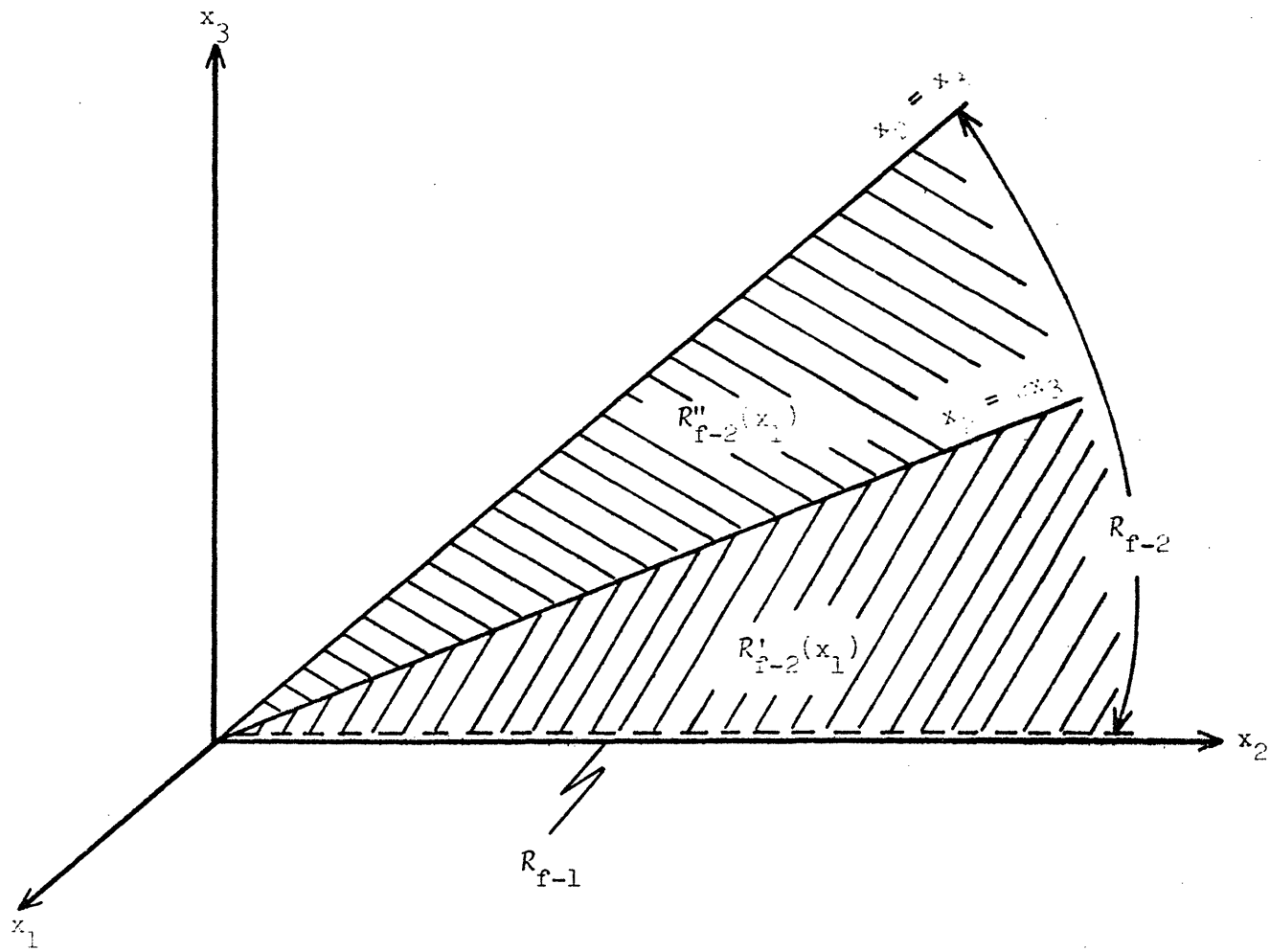

Figure 10 - The subregions $R'_{f-2}(x_1)$ and $R''_{f-2}(x_1)$ of the feedback control region R_{f-2}.

We now want to allow x_1 to leave the boundary backward in time at some $t_{f-2} < t_{f-1}$; that is, allow the state to leave from R_{f-2}. This is achieved by rotating the two dimensional Hamiltonian hyperplane $H_{f-3}(t_{f-2})$: $Z = \lambda_1(t_{f-2})y_1 + \lambda_2(t_{f-2})y_2 + \lambda_3(t_{f-2})y_3$ about $H_{f-2}(t_{f-2})$ until it touches Y on a face in the positive orthant of y_1. We distinguish the following cases:

(i) If $\lambda_3(t_{f-2}) < \lambda_2(t_{f-2})$, then $H_{f-3}(t_{f-2})$ is rotated to touch the edge labeled e' in Figure 8(b). The point $\underline{y}'$ becomes the new set of operating points Y_{f-3}.

(ii) If $\lambda_3(t_{f-2}) = \lambda_2(t_{f-2})$, then $H_{f-3}(t_{f-2})$ is rotated to touch the face labeled F_1 in Figure 8(c). Subsequent rotation of H_{f-3} causes the point $\underline{y}''$ of Figure 8(c) to become the new set of operating points Y_{f-3}.

(iii) If $\lambda_3(t_{f-2}) > \lambda_2(t_{f-2})$, then $H_{f-3}(t_{f-2})$ is rotated to touch the edge labeled e" in Figure 8(c). The point $\underline{y}''$ becomes the new set of operating points Y_{f-3}.

If we denote the time at which λ_2 equals λ_3 by τ', then from Figure 10 we easily determine that $x_2(\tau') = 2x_3(\tau')$. Therefore, we divide the region R_{f-2} into two subregions as depicted in Figure 10: $R'_{f-2}(x_1)$ is that portion of R_{f-2} beneath the line $x_2 = 2x_3$, not including $x_2 = 2x_3$; $R''_{f-2}(x_1)$ is that portion of R_{f-2} above and including the line $x_2 = 2x_3$. When the state leaves $R'_{f-2}(x_1)$ the new set of operating points is $Y_{f-3} = \underline{y}'$. On the other hand, when the state leaves $R''_{f-2}(x_1)$ the new set of operating points is $Y_{f-3} = \underline{y}''$.

□ Example 2

C. Global Optimality

A simple example is now presented to illustrate the geometrical interpretation for determining if a solution to the constrained optimization problem is globally optimal. In the particular situation presented, global optimality does *not* hold.

Example 3

Once again consider the network topology of Figure 5.

For the purpose of this example, we limit attention to the state variables x_3^1 and x_2^1 and consider the cost function

$$J = \int_{t_o}^{t_f} [2x_2^1(t) + x_3^1(t)]dt \ . \qquad (28)$$

The y-space constraint figure is presented in Figure 11.

We begin by letting x_2^1 leave the boundary backward in time at t_f. Then the constrained optimization problem in y-space calls for the maximization of the zero dimensional Hamiltonian hyperplane $H_{f-1}(\tau)$: $Z = \lambda_2^1(\tau)y_2^1$ over the constraint region Y_{f-1} depicted in Figure 11. The trajectory for λ_2^1 is shown in Figure 12. The solution to the constrained optimization problem is Y_{f-1}: $y_2^1 = 1.5$, $y_3^1 = 0$, as illustrated in Figure 11. Now, for any $\tau < t_f$ let us see if there exists some value of $\lambda_3^1(\tau)$ such that the global Hamiltonian hyperplane $H(\tau)$: $Z = \lambda_2^1(\tau)y_2^1 + \lambda_3^1(\tau)y_3^1$ is tangent to Y at Y_{f-1}. From Figure 11 it is seen that the *only* possible such value is $\lambda_3^1(\tau) = \lambda_2^1(\tau)$. However, from (24) and the transversality condition (equations (19) of [1]) we have $\lambda_3^1(\tau) \leq \frac{1}{2}\lambda_2^1(\tau)$ as depicted in Figure 12. Therefore, the candidate operating point Y_{f-1} obtained from the constrained optimization is *not* a global optimum.

□ Example 3.

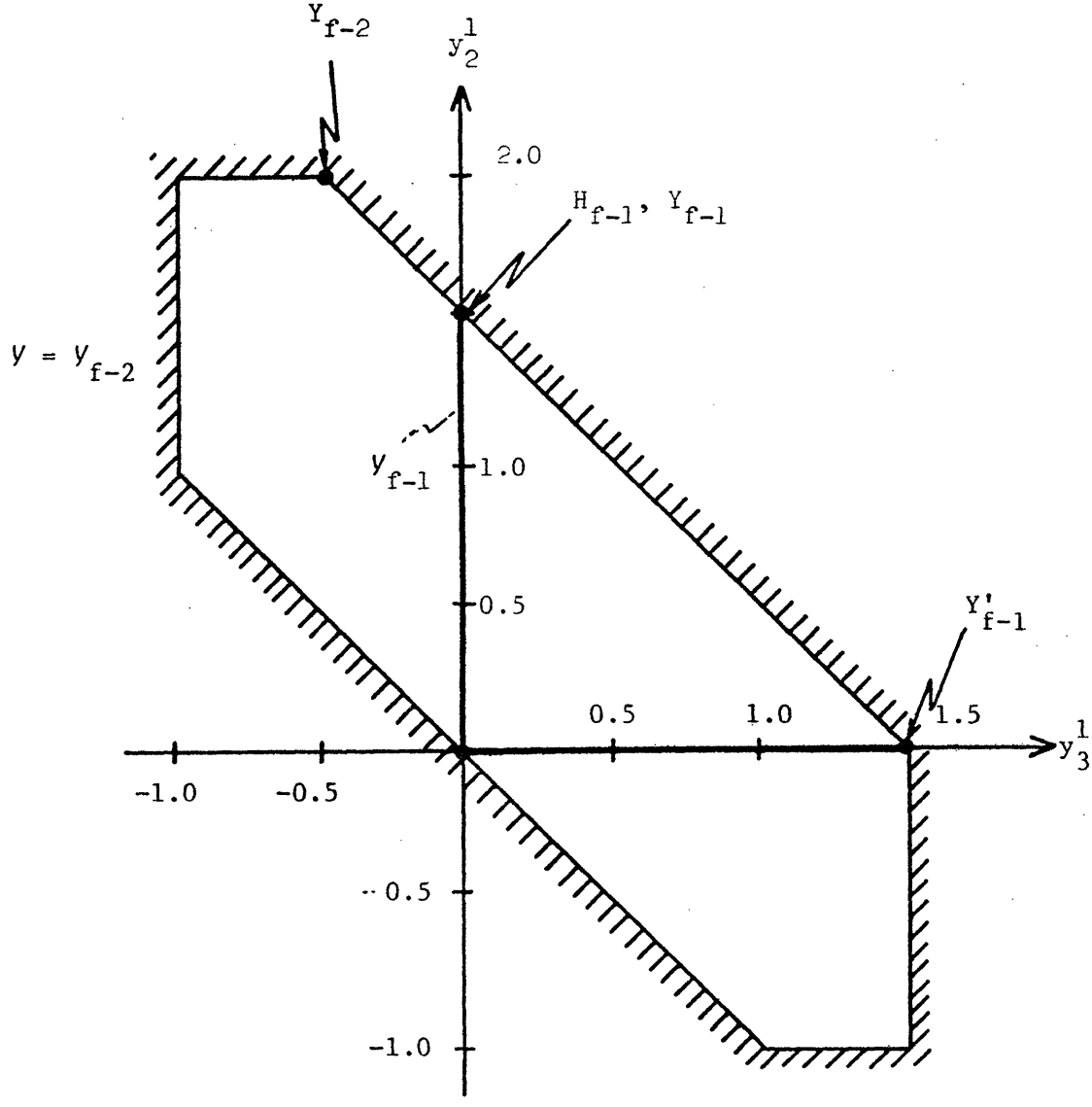

Figure 11 - The y-space constraint figure for Examples 3 and 4.

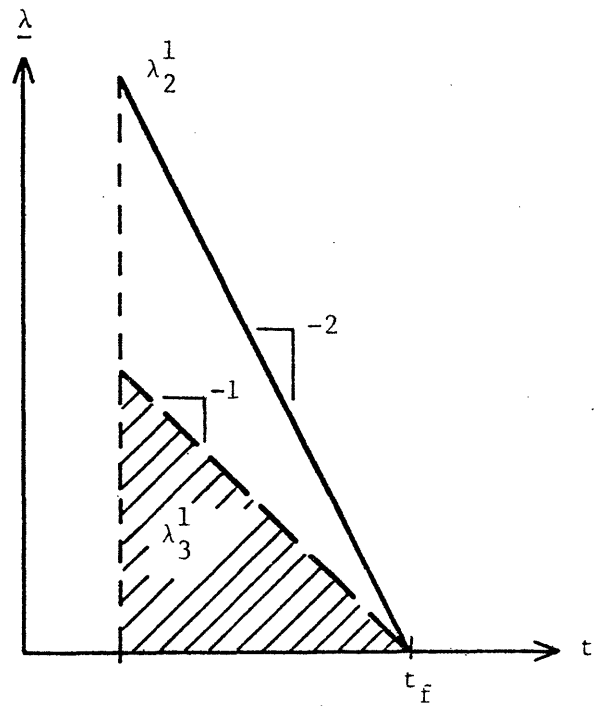

Figure 12 - Costate Trajectories for Example 3.

D. Off-the Boundary Assumption

Example 4 demonstrates the geometrical interpretation for testing the validity of the off-the-boundary assumption for a situation in which the assumption does *not* hold.

Example 4

We once again refer to the network topology of Figure 5 and concern ourselves with the state variable x_2^1 and x_3^1 as in Example 3. The y-space constraint figure appears as in Figure 11, and the cost functional is taken as (28).

In example 3, we attempted to allow x_2^1 to leave the boundary backward in time at t_f and discovered that such a trajectory cannot be globally optimal. We now try letting x_3^1 leave the boundary backward in time at t_f. The trajectory for λ_3^1 is shown in Figure 13 and the non-break solution to the constrained optimization problem is readily seen to be Y'_{f-1}: $y_2^1 = 0$, $y_3^1 = 1.5$ from Figure 11. This solution is globally optimal when $\lambda_2^1(\tau)$ is taken to be equal to $\lambda_3^1(\tau)$. This value of $\lambda_2^1(\tau)$ satisfies (24) with equality since the transversality condition requires $\lambda_2^1(t_f) = 0$.

Suppose we now allow x_2^1 to leave the boundary backward in time at the arbitrary boundary junction time $t_{f-1} < t_f$. It is readily seen that the leave-the-boundary value of $\lambda_2^1(t_{f-1})$ is achieved when it is equal to $\lambda_3^1(t_{f-1})$. Once x_2^1 leaves the boundary backward in time its costate travels as indicated in Figure 13. Since $\lambda_2^1(\tau) > \lambda_3^1(\tau)$ for $\tau < t_{f-1}$, then the only globally optimizing operating point in this situation is Y_{f-2}: $y_2^1 = 2.0$, $y_3^1 = -0.5$. Hence, the optimal slope of x_3^1 forward in time is +0.5 and therefore x_3^1 *must return to the boundary backward in time.*

□ Example 4

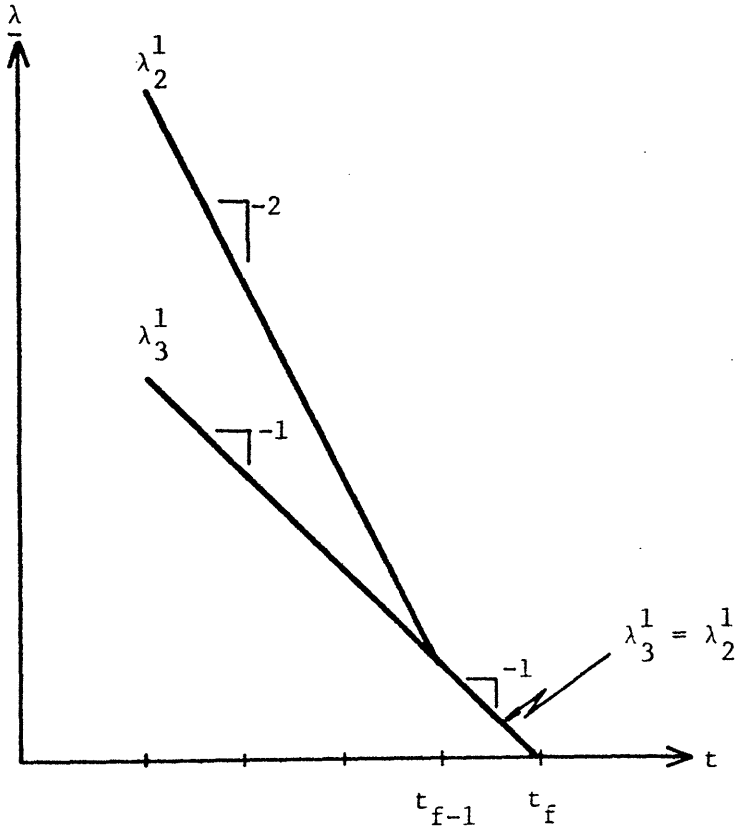

Figure 13 - Costate trajectories for Example 4.

V. DISCUSSION AND CONCLUSIONS

In this paper a geometrical interpretation has been presented which provides the principles for coping with the problems of the Constructive Dynamic Programming Algorithm listed in Section VI of [1]. However, it is not currently known how this approach may be applied to construct a numerical version of the algorithm for general network problems. The fundamental complication is that the geometrical interpretation requires explicit knowledge of the y-space constraint figure and although we may readily find the appropriate constraints for simple cases of three dimensions or less (as in Examples 1-4), it is not understood how this may be accomplished for problems of arbitrarily high dimension.

Another complication is that it is desirable to determine the validity of the "off-the-boundary assumption" *a priori* for all possible optimal trajectories corresponding to a given network problem. Whether or not this assumption holds for a given problem is a basic property which determines the applicability of the Constructive Dynamic Programming Algorithm. No technique is currently known for the *a priori* assessment of the validity of this assumption for general network problems.

Nonetheless, the geometrical interpretation presents several significant benefits. To begin it provides a powerful conceptual tool for gaining insight into the necessary conditions of optimality associated with continuous linear optimal control problems with linear state and control variable inequality constraints. The insight which is gained may be of interest *exclusive* of its applicability to the Constructive Dynamic Programming Algorithm itself. For example, we have formulated a compact geometrical condition for determining the uniqueness or nonuniqueness of the costate variables, and

have used it to demonstrate the potential *nonuniqueness of costate variables at times when their corresponding state variables are travelling on interior arcs* (Example 1). This is a most interesting property which characterizes linear state constrained optimal control problems. Although it is well known that nonuniqueness of the costate variables may occur in nonlinear state constrained optimal control problems (see for example [3] and [4]), it is limited to those costate variables corresponding to state variables travelling on boundary arcs or at boundary junctions.

From the point of view of Constructive Dynamic Programming Algorithm, the geometrical interpretation provides the theoretical framework for recognizing and proving simplifications which arise in special network problems. In a forthcoming paper by the authors (Part III of this series) the geometrical interpretation is applied to the case of single destination networks with all unity weightings in the cost functional to prove several simplifications which permit a numerical formulation of the Constructive Dynamic Programming Algorithm for that problem. Briefly, these simplifications are:

1. Uniqueness of the leave-the-boundary costates.
2. Exactly one subregion per every feedback control region.
3. Solutions to the constrained optimization problems are always globally optimal.
4. An optimal control always exists without breakpoints between boundary junctions.

References

[1] Moss, F.H. and Segall, A., "An Optimal Control Approach to Dynamic Routing in Data Communication Networks, Part I: Principles", submitted to *IEEE Trans. Autom. Control*.

[2] Segall, A., "The Modelling of Adaptive Routing in Data-Communication Networks", *IEEE Trans. Comm.*, Vol. COM-25, No. 1, pp. 85-95, January 1977.

[3] Bryson, A.E., Denham, W.F. and Dreyfus, S.E., "Optimal Programming Problems with Inequality Constraints I: Necessary Conditions for Extremal Solutions", *AIAA J.* 1, No. 11, 2544-2550, 1963.

[4] Jacobson, D.H., Lele, M.M. and Speyer, J.L., "New Necessary Conditions of Optimality for Control Problems with State-Variable Inequality Constraints", *J. of Math. Anal. and Appl.*, Vol. 35, No. 2, 255-284, August 1971.